

STATIC BENDING ANALYSIS OF ANNULAR NANOPLATES RESTING ON ELASTIC FOUNDATION USING NONLOCAL ELASTICITY THEORY

Le Pham Binh^{*}, Doan Trac Luat, Le Minh Thai, Tran Trung Thanh

Le Quy Don Technical University

Abstract

This article presents an application of finite element algorithm for static bending analysis of the functionally graded porous (FGP) annular nanoplate resting on the elastic foundation (EF) using nonlocal elasticity theory. The FGP materials with two parameters are the volume fraction index (k) and the porosity volume fraction (ξ) was used in two cases of even and uneven porosity. The EF includes Winkler-stiffness (k_1) and Pasternak-stiffness (k_2). For the first time, the stress and displacement of the FGP annular nanoplates are established using an eight-node plate element (Q8). Numerical results of the proposed method are compared with those of published works to verify the accuracy and reliability. Furthermore, the impacts of some factors such as the elastic foundation and material on the static bending of FGP nanoplates resting on the EF are studied in detail.

Keywords: FGM; static bending; nanoplates; nonlocal elasticity theory.

1. Introduction

Nowadays, nanostructures have been widely applied in nanoelectromechanical systems such as thin-film elements, nanosheet resonators, and gas sensors due to their exceptional mechanical, thermal, and electrical properties. Therefore, the research on nanostructures has always been deeply interested by scientists around the world.

There are many theories that have been proposed to calculate nano-structures such as the modified couple stress theory [1], the strain gradient theory [2], and the nonlocal theory [3, 4]. Among these theories, the nonlocal theory is used popularly in the literature for simplicity and accuracy. For example, Li et al. [5] developed a new nonlocal model to solve the static and dynamic problems for circular elastic nano-solids. Ansari et al. [6, 7] used nonlocal theory to consider the free vibration of a single-layered graphene plate. In [7], Arash and co-workers commented about nonlocal theory in modeling carbon nanotubes and graphene. Farajpour et al. [8] studied thermomechanical vibration of graphene plates including surface effects by decoupling the nonlocal

^{*} Email: lephambinh@lqdtu.edu.vn

elasticity equations. Jalali et al. [9] used molecular dynamics combining with nonlocal elasticity approaches to investigate the effect of out-of-plane defects on vibration analysis of graphene. In addition, the nonlocal theory employed to investigate the various performances of nanoplates is also shown in [10].

In the case of nanostructures resting on the EF, some typical works as Wang and Li [11] computed the static bending of the nanoplates resting on the EF. Narendar and Gopalakrishnan et al. [12] studied the wave dispersion of a single-layered graphene sheet embedded in an elastic polymer matrix. Pouresmaeli et al. [13] investigated the vibration behaviors of nanoplates placed on a viscoelastic medium. Sobhy [14] used an analytical method based on nonlocal theory to examine static bending, free vibration, mechanical buckling, and thermal buckling of functionally graded material (FGM) nanoplates lying on the EF. Le et al. [15] employed the FEM based on nonlocal elasticity theory to examine static bending of L-shape nanoplates.

Basically, porosity reduces the stiffness of the structure, however with engineering properties such as lightweight, excellent energy-absorbing capability, great thermal resistant properties, etc, they still have been widely applied in various fields including aerospace, automotive industry, and civil engineering. Recently, porous nanostructures are also widely used for potential applications in various fields such as electronic devices, sensors and solar cells [16-18].

According to the best of the authors' knowledge, the static bending analysis of FGP annular nanoplates resting on EF has been not published yet. This motivates us to develop the eight-node quadrilateral (Q8) element combining with the nonlocal theory to accurately describe the stress-strain and displacement field of the FGP annular nanoplate resting on the EF. The accuracy and reliability of the present approach are verified by comparing numerical results with other previous publications. Moreover, the effects of geometry parameters and material properties on the static bending of FGP nanoplates are examined in detail.

2. Governing equations

2.1. The FGP annular nanoplate

Consider an annular nanoplate as shown in Fig. 1.

The FGP materials with a variation of two constituents and two different distributions of porosity through-thickness are presented as [12]:

$$\text{Case 1: } P(z) = P_m + (P_c - P_m) \left(\frac{z}{h} + 0,5 \right)^k - \frac{\xi}{2} (P_c + P_m) \quad (1)$$

$$\text{Case 2: } P(z) = P_m + (P_c - P_m) \left(\frac{z}{h} + 0,5 \right)^k - \frac{\xi}{2} (P_c + P_m) \left(1 - \frac{2|z|}{h} \right) \quad (2)$$

where P represents the effective material property such as Young's modulus E , mass density ρ , and Poisson's ratio ν . k is the volume fraction index, ξ ($\xi \leq 1$) represents the porosity volume fraction. Subscripts m and c denotes the metallic and ceramic constituents, respectively.

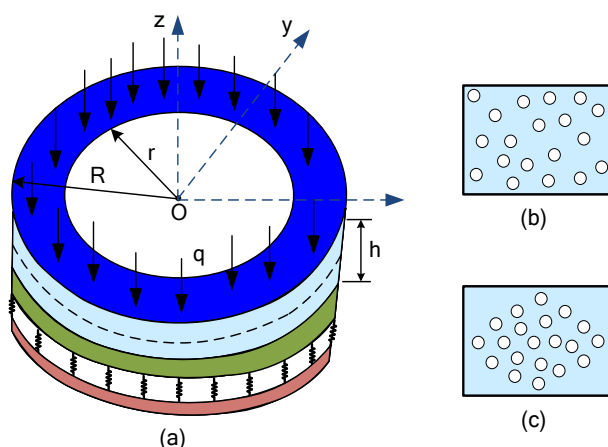


Fig. 1. The FGP annular nanoplate resting on the EF
(a) Annular nanoplate, (b) Even porosity, (c) Uneven porosity.

2.2. Nonlocal elasticity theory

According to the nonlocal theory, the stress-strain relation is determined by [4]

$$\boldsymbol{\sigma} - \mu \nabla^2 \boldsymbol{\sigma} = \mathbf{Q} \quad (3)$$

in which: $\mu = (e_0 l)^2$ is nonlocal factor, l is an internal characteristic length and e_0 is a constant. \mathbf{Q} is the stress tensor at a point that is calculated follows the local theory. Note that, when $l = 0$ ($\mu = 0$), the nonlocal theory will become the classical plate theory. $\nabla^2 = \left(\frac{\partial^2}{\partial x^2} + \frac{\partial^2}{\partial y^2} \right)$ is the Laplacian operator and hence, the small-scale effect depends on the atomic or molecular mechanical/electrical/chemical characteristics, i.e. bond strength, atomic spacing, atomic potential, and density are taken into account.

2.3. The displacement field

According to the first-order shear deformation theory (FSDT), the displacement field of the FGP nanoplate is given by:

$$u(x, y, z) = u_0(x, y) + z\theta_y(x, y); v(x, y, z) = v_0(x, y) + z\theta_x(x, y); w(x, y, z) = w_0(x, y) \quad (4)$$

with u_0, v_0, w_0 are the displacement components at the mid-plane ($z = 0$) along x, y, z -axis; θ_x, θ_y are the angle of rotation of the middle surface via the y and x -axis, respectively.

2.4. The strain vector

The strain vector of the plate is defined according to the displacement field as follows [12]:

$$\boldsymbol{\varepsilon} = \begin{Bmatrix} \varepsilon_{xx} \\ \varepsilon_{yy} \\ \varepsilon_{xy} \\ \varepsilon_{xz} \\ \varepsilon_{yz} \end{Bmatrix} = \begin{Bmatrix} u_{,x} \\ v_{,y} \\ u_{,y} + v_{,x} \\ w_{,x} + u_{,z} \\ w_{,y} + v_{,z} \end{Bmatrix} = \begin{Bmatrix} u_{0,x} \\ v_{0,y} \\ u_{0,y} + v_{0,x} \\ v_{0,x} + \theta_x \\ w_{0,y} + \theta_y \end{Bmatrix} + z \begin{Bmatrix} \theta_{x,x} \\ \theta_{y,y} \\ \theta_{x,y} + \theta_{y,x} \\ 0 \\ 0 \end{Bmatrix} \quad (5)$$

$$\boldsymbol{\varepsilon} = \{\boldsymbol{\varepsilon}_1 \quad \boldsymbol{\varepsilon}_2\}^T = \{\boldsymbol{\varepsilon}_1^0 + z\boldsymbol{\varepsilon}_1^1 \quad \boldsymbol{\varepsilon}_2^0\}^T \quad (6a)$$

with

$$\boldsymbol{\varepsilon}_1 = \begin{Bmatrix} \varepsilon_{xx} \\ \varepsilon_{yy} \\ \varepsilon_{xy} \end{Bmatrix}; \boldsymbol{\varepsilon}_2 = \begin{Bmatrix} \varepsilon_{xz} \\ \varepsilon_{yz} \end{Bmatrix}; \boldsymbol{\varepsilon}_1^0 = \begin{Bmatrix} u_{0,x} \\ v_{0,y} \\ u_{0,y} + v_{0,x} \end{Bmatrix}; \boldsymbol{\varepsilon}_1^1 = \begin{Bmatrix} \theta_{x,x} \\ \theta_{y,y} \\ \theta_{x,y} + \theta_{y,x} \end{Bmatrix}; \boldsymbol{\varepsilon}_2^0 = \begin{Bmatrix} w_{0,x} + \theta_x \\ w_{0,y} + \theta_y \end{Bmatrix} \quad (6b)$$

2.5. The stress-strain relation

$$\mathbf{Q} = \mathbf{D} \cdot \boldsymbol{\varepsilon} \quad (7)$$

$$\mathbf{D} = \begin{bmatrix} \mathbf{D}_b & \mathbf{0}_{3 \times 2} \\ \mathbf{0}_{2 \times 3} & \mathbf{D}_s \end{bmatrix}; \mathbf{D}_b = \begin{bmatrix} C_{11} & C_{12} & 0 \\ & C_{22} & 0 \\ sym & & C_{66} \end{bmatrix}; \mathbf{D}_s = \begin{bmatrix} C_{55} & 0 \\ 0 & C_{44} \end{bmatrix} \quad (8)$$

$$C_{11} = C_{22} = \frac{E}{(1-\nu^2)}; C_{12} = \frac{\nu E}{(1-\nu^2)}; C_{66} = C_{55} = C_{44} = \frac{E}{2(1+\nu)} \quad (9)$$

The equation represents the relationship between the internal forces and the deformation components are written in the form:

$$\{N_{xx} \quad N_{yy} \quad N_{xy}\}^T = \mathbf{A}\boldsymbol{\varepsilon}_1^0 + \mathbf{B}\boldsymbol{\varepsilon}_1^1; \{M_{xx} \quad M_{yy} \quad M_{xy}\}^T = \mathbf{B}\boldsymbol{\varepsilon}_1^0 + \mathbf{X}\boldsymbol{\varepsilon}_1^1; \{Q_{xz} \quad Q_{yz}\}^T = \mathbf{A}^s \boldsymbol{\varepsilon}_2^0 \quad (10)$$

where $\mathbf{A}; \mathbf{B}; \mathbf{X}; \mathbf{A}^s$ are determined as follow:

$$(\mathbf{A}; \mathbf{B}; \mathbf{X}) = \int_{-h/2}^{h/2} \mathbf{D}_b \cdot (1; z; z^2) dz; \mathbf{A}^s = \frac{5}{6} \int_{-h/2}^{h/2} \mathbf{D}_s \cdot dz \quad (11)$$

2.6. The plate element

The eight-node plate element is used. Each node has five degrees of freedom. The nodal displacement vector can be defined as follows:

$$\mathbf{d}_e = [\mathbf{d}_1^T \quad \mathbf{d}_2^T \quad \mathbf{d}_3^T \quad \mathbf{d}_4^T \quad \mathbf{d}_5^T \quad \mathbf{d}_6^T \quad \mathbf{d}_7^T \quad \mathbf{d}_8^T]^T \quad (12)$$

The displacements at the node i ($i = 1 \div 8$) of element are expressed as

$$\mathbf{d}_i = \{u_{0i} \quad v_{0i} \quad w_{0i} \quad \varphi_{xi} \quad \varphi_{yi}\} \quad (13)$$

The displacements field in the plate element is interpolated through the displacement node as

$$u_0 = \mathbf{N}_u \cdot \mathbf{d}_e; v_0 = \mathbf{N}_v \cdot \mathbf{d}_e; w_0 = \mathbf{N}_w \cdot \mathbf{d}_e; \varphi_x = \mathbf{N}_{\varphi_x} \cdot \mathbf{d}_e; \varphi_y = \mathbf{N}_{\varphi_y} \cdot \mathbf{d}_e \quad (14)$$

where $\mathbf{N}_u, \mathbf{N}_v, \mathbf{N}_w, \mathbf{N}_{\varphi_x}, \mathbf{N}_{\varphi_y}$ are the shape functions:

$$\begin{cases} \mathbf{N}_u = [\mathbf{N}_1^{(1)} & \mathbf{N}_2^{(1)} & \dots & \mathbf{N}_7^{(1)} & \mathbf{N}_8^{(1)}]; \mathbf{N}_v = [\mathbf{N}_1^{(2)} & \mathbf{N}_2^{(2)} & \dots & \mathbf{N}_7^{(2)} & \mathbf{N}_8^{(2)}]; \\ \mathbf{N}_w = [\mathbf{N}_1^{(3)} & \mathbf{N}_2^{(3)} & \dots & \mathbf{N}_7^{(3)} & \mathbf{N}_8^{(3)}]; \mathbf{N}_{\varphi_x} = [\mathbf{N}_1^{(4)} & \mathbf{N}_2^{(4)} & \dots & \mathbf{N}_7^{(4)} & \mathbf{N}_8^{(4)}]; \\ \mathbf{N}_{\varphi_y} = [\mathbf{N}_1^{(5)} & \mathbf{N}_2^{(5)} & \dots & \mathbf{N}_7^{(5)} & \mathbf{N}_8^{(5)}]. \end{cases} \quad (15)$$

The matrices $\mathbf{N}_i^{(j)}$ ($j = 1 \div 5$) are given by

$$\begin{cases} \mathbf{N}_i^{(1)} = [\psi_i & 0 & 0 & 0 & 0]; \\ \mathbf{N}_i^{(2)} = [0 & \psi_i & 0 & 0 & 0]; \\ \mathbf{N}_i^{(3)} = [0 & 0 & \psi_i & 0 & 0]; \\ \mathbf{N}_i^{(4)} = [0 & 0 & 0 & \psi_i & 0]; \\ \mathbf{N}_i^{(5)} = [0 & 0 & 0 & 0 & \psi_i]. \end{cases} \quad (16)$$

where ψ_i is the Lagrange interpolation function.

The element stiffness matrix is determined by

$$\mathbf{K}_e = \mathbf{K}_e^p + \mathbf{K}_e^f \quad (17)$$

with $\mathbf{K}_e^p, \mathbf{K}_e^f$ are the plate element stiffness matrix, and the foundation element stiffness matrix, respectively. In which

$$\mathbf{K}_e^p = \int_{S_e} \left(\begin{bmatrix} \mathbf{B}_1^T & \mathbf{B}_2^T \end{bmatrix} \begin{bmatrix} \mathbf{A} & \mathbf{B} \\ \mathbf{B} & \mathbf{X} \end{bmatrix} \begin{bmatrix} \mathbf{B}_1 \\ \mathbf{B}_2 \end{bmatrix} + \mathbf{B}_3^T \mathbf{A}^s \mathbf{B}_3 \right) dx dy \quad (18)$$

$$\mathbf{K}_e^f = \int_{S_e} k_1 \left(\mathbf{N}_w^T \mathbf{N}_w + \mu \left(\mathbf{N}_{w,x}^T \mathbf{N}_{w,x} + \mathbf{N}_{w,y}^T \mathbf{N}_{w,y} \right) \right) + k_2 \left(\mathbf{N}_{w,x}^T \mathbf{N}_{w,x} + \mathbf{N}_{w,y}^T \mathbf{N}_{w,y} \right) + \mu \left(\mathbf{N}_{w,xx}^T \mathbf{N}_{w,xx} + \mathbf{N}_{w,yy}^T \mathbf{N}_{w,yy} + \mathbf{N}_{w,xy}^T \mathbf{N}_{w,xy} + \mathbf{N}_{w,yx}^T \mathbf{N}_{w,yx} \right) dx dy \quad (19)$$

$$\text{where } \mathbf{B}_1 = \begin{bmatrix} \mathbf{N}_{u,x} \\ \mathbf{N}_{v,y} \\ \mathbf{N}_{u,x} + \mathbf{N}_{v,y} \end{bmatrix}; \mathbf{B}_2 = \begin{bmatrix} \mathbf{N}_{\varphi x,x} \\ \mathbf{N}_{\varphi y,y} \\ \mathbf{N}_{\varphi x,y} + \mathbf{N}_{\varphi y,x} \end{bmatrix}; \mathbf{B}_3 = \begin{bmatrix} \mathbf{N}_{w,x} + \mathbf{N}_{\varphi x} \\ \mathbf{N}_{w,y} + \mathbf{N}_{\varphi y} \end{bmatrix} \quad (20)$$

$$\mathbf{N} = \begin{bmatrix} \mathbf{N}_u^T & \mathbf{N}_v^T & \mathbf{N}_w^T & \mathbf{N}_{\varphi x}^T & \mathbf{N}_{\varphi y}^T \end{bmatrix} \quad (21)$$

$$\text{The element force vector is given as follows: } \mathbf{F}_e = \int_S p(1 - \mu \nabla^2) \mathbf{N}_w^T dS \quad (22)$$

with $\mathbf{N}_w = [0 \ 0 \ N_1 \ 0 \ 0, \dots, 0 \ 0 \ N_8 \ 0 \ 0]$.

$$\text{For the static problem: } \mathbf{K} \cdot \mathbf{d} = \mathbf{F} \quad (23)$$

in which $\mathbf{K}, \mathbf{F}, \mathbf{d}$ are the global stiffness matrix, the global force vector, and the global displacement vector. They are gathered from the element stiffness matrix, the element force vector, and the element displacement vector. The program is coded in the Matlab environment.

3. Accuracy study

Firstly, we consider simple support (SSSS) FGM square nanoplates with geometry parameters: $a = b = 10 \text{ nm}$, $h = a/10$; and material properties: metal (Al) $E_1 = 70 \text{ GPa}$, $\rho_1 = 2702 \text{ kg/m}^3$, and ceramic (Al_2O_3) $E_2 = 380 \text{ GPa}$, $\rho_2 = 3800 \text{ kg/m}^3$, $\nu = 0.3$ is fixed. Herein, dimensionless quantities are introduced by

$$w^* = \frac{100E_2h^3}{q_0a^4} w, \sigma_{xx}^* = \frac{10h}{q_0a} \sigma_{xx}, \sigma_{xy}^* = \frac{10h}{q_0a} \sigma_{xy}, K_1 = \frac{k_1a^4}{H}, K_2 = \frac{k_2a^2}{H}, H = \frac{E_2h^3}{12(1-\nu^2)} \quad (24)$$

As exhibited in Table 1, the present results are in good agreement with an analytical method of Sobhy [14]. It means that the present method is highly reliable.

Table 1. The displacement and stress of nanoplates resting on the EF ($k = 0, K_2 = 0$).

Method	K_1	$\mu = 0$		$\mu = 4$	
		w^*	σ_{xx}^*	w^*	σ_{xx}^*
[14]	0	2.9603	19.9550	5.2977	35.7108
	100	2.3290	15.6991	3.5671	24.0455
Present	0	2.9600	19.8990	5.2971	35.6106
	100	2.3288	15.6555	3.5669	23.9791

4. Numerical results

Secondly, the FGP annular nanoplates (as Fig. 1) material properties as in section 3 and geometric dimensions $R = 5$ nm, $r = 2.5$ nm, $h = 1$ nm. The FGP annular nanoplate subjected to uniformly load p_0 in perpendicular directions. The deformation field of the FGP annular nanoplate is indicated in Figs. 2a, 2b. The stresses of A-point through the thickness of the FGP annular nanoplate is presented in Figs. 2c, 2d. It can be seen that the law of stress distribution according to the thickness of the plate at a point is consistent with the law of effective mechanical properties of FGM materials.

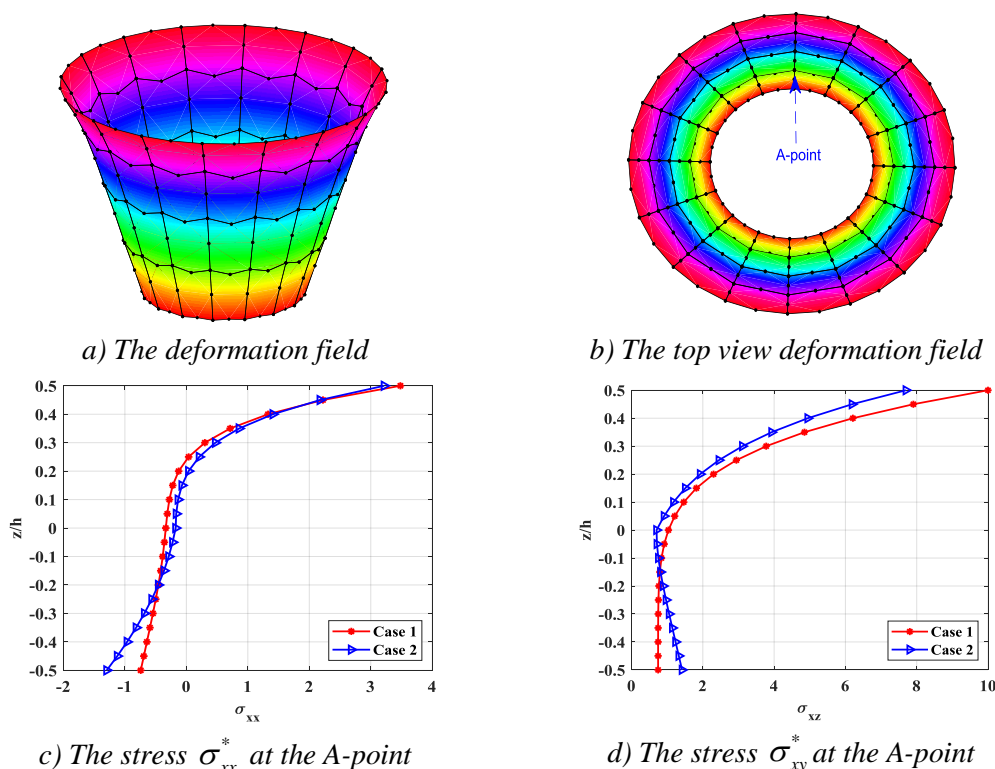


Fig. 2. The deformation and stresses of the SSSS FGP annular nanoplate ($k = 5$, $\xi = 0.1$, $\mu = 4$, $K_1 = 100$, $K_2 = 10$).

4.1. Effect of the volume fraction index k

Next, the volume fraction index k gets value from 0 to 100. The SSSS FGP annular nanoplate with porosity volume fraction $\xi = 0.1$, nonlocal factor $\mu = 4$. The stiffness of foundation: $K_1 = 100$, $K_2 = 50$. From Fig. 3, it can be concluded that when k increases lead to displacement increase due to stiffness of the nanoplate decrease. The displacement of the nanoplate decreases rapidly when k increases from 0 to 10. We also find that the FGP annular nanoplates with porosity distribution case 2 are harder than case 1. Note that, k is larger the nanoplate becomes metal-rich and thus the nanoplate's stiffness decreases.

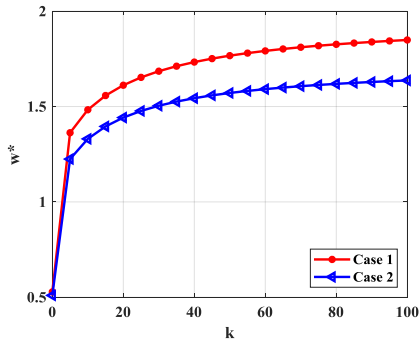


Fig. 3. The maximum displacement of the SSSS FGP annular nanoplate versus volume fraction index k .

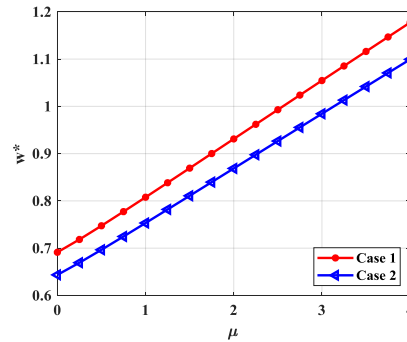


Fig. 4. The maximum displacement of the SSSS FGP annular nanoplate versus nonlocal factor μ .

4.2. Effect of the nonlocal factor μ

In this survey, authors choose the nonlocal factor in range $\mu = 0 \div 4$ with $\mu = 0$ is the classical plate. The SSSS annular FGP nanoplate with porosity volume fraction $\xi = 0.1$, volume fraction index $k = 5$. The stiffness of foundation: $K_1 = 100$, $K_2 = 50$. It can be found that μ increases make the displacement increase due to increase of nonlocal factor lead to reduce stiffness of the FGP annular nanoplate (see Fig. 4).

4.3. Effect of the stiffness of foundation

Finally, in order to consider the influences of the stiffness of foundation on static bending of the FGP annular nanoplate, we change K_1 from 0 to 500, and K_2 from 0 to 50 with respect to $k = 5$, $\xi = 0.2$, and nonlocal factor $\mu = 4$. From the numerical results show in Fig. 5, we observe that when increasing K_1 and K_2 leads to a decrease in the displacement of nanoplates due to the foundation make the stiffness of FGP annular nanoplates increase, and Pasternak foundation supports strongly than Winkler foundation.

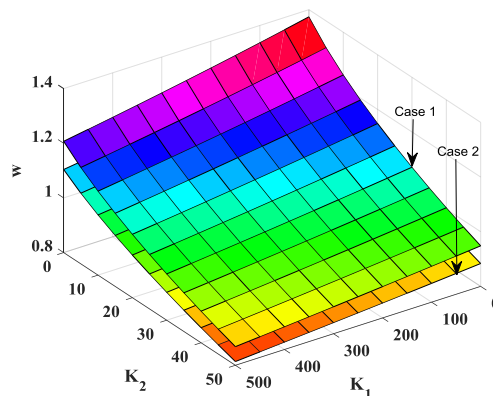


Fig. 5. The displacement of the FGP annular nanoplate versus K_1 and K_2 .

5. Conclusions

In this article, the static analysis of the FGP annular nanoplate is studied by using the FEM and nonlocal theory. The obtained numerical results of static bending of the present approach are compared to other available solutions. From the proposed formulation and the numerical results, we can withdraw some following points:

- Using the FEM will be convenient in modeling and meshing. Especially, with structures are not symmetrical (L-shape, Annular-shape).
- The material parameters and the porosity distribution of the FG material effect significantly the static bending of FGP annular nanoplates.
- Numerical results in the present work are useful for the calculation, design of FGP annular nanoplates in engineering and technologies.
- The present approach can be developed to investigate static bending of the FGP nanoplate with different shapes subjected to other loads.

References

- [1] Yang F, Chong ACM, Lam DCC, Tong P., "Couple stress based strain gradient theory for elasticity", *Int J Solids Struct* 2002, 39: 2731-43.
- [2] Aifantis EC., "Strain gradient interpretation of size effects", *Int J Fract* 1999; 95:1-4.
- [3] A. C. Eringen, "On differential equations of nonlocal elasticity and solutions of screw dislocation and surface waves", *Journal of Applied Physics*, Vol. 54, No. 9, pp. 4703-4710, 1983.
- [4] A.C. Eringen, *Nonlocal Continuum Field Theories*, Springer: New York (NY), 2002.
- [5] C. Li, C.W. Lim, J. Yu, "Twisting statics and dynamics for circular elastic nanosolids by nonlocal elasticity theory", *Acta Mechanica Solida Sinica*, Vol. 24, No. 6, pp. 484-94, 2011.
- [6] R. Ansari, S. Sahmani, B. Arash, "Nonlocal plate model for free vibrations of single-layered graphene sheets", *Physica Letter A*, Vol. 375, No. 1, pp. 53-62, 2010.
- [7] B. Arash, Q. Wang, "A review on the application of nonlocal elastic models in modeling of carbon nanotubes and graphenes", *Computational Materials Science*, Vol. 51, No. 1, pp. 303-313, 2012.
- [8] S. R. Asemi, A. Farajpour, "Decoupling the nonlocal elasticity equations for thermomechanical vibration of circular graphene sheets including surface effects", *Physica E*, Vol. 60, pp. 80-90, 2010.
- [9] S. K. Jalali, E. Jomehzadeh, N. M. Pugno, "Influence of out-of-plane defects on vibration analysis of graphene: Molecular Dynamics and Nonlocal Elasticity approaches", *Superlattices and Microstructures*, Vol. 91, pp. 331-344, 2016.
- [10] R. Ahababaei, J. N. Reddy, "Nonlocal third-order shear deformation plate theory with application to bending and vibration of plate", *Journal of Sound and Vibration*, Vol. 326, No. 1-2, pp. 277-289, 2009.

- [11] Y. Z. Wang, F.M.Li, "Static bending behaviors of nano-plate embedded in elastic matrix with small scale effects", *Mechanics Research Communications*, Vol. 41, pp. 44-48, 2012.
- [12] S. Narendar, S. Gopalakrishnan S, "Nonlocal continuum mechanics based ultrasonic flexural wave dispersion characteristics of a monolayer graphene embedded in polymer matrix", *Composites Part B: Engineering*, Vol. 43, No. 8, pp. 3096-3103, 2012.
- [13] S. Poursmaeeli, E. Ghavanloo, S. A. Fazelzadeh, "Vibration analysis of viscoelastic orthotropic nano-plates resting on viscoelastic medium", *Composite Structures*, Vol. 96, pp. 405-410, 2013.
- [14] Mohammed Sobhy, "A comprehensive study on FGM nanoplates embedded in an elastic medium", *Composite Structures*, Vol. 134, pp. 966-980, 2015.
- [15] Le. P. B, Doan. T. L, Le. M. T, Tran. T. T, "Nonlocal elasticity theory for static bending analysis of nanoplates resting on elastic foundation", *Collection of Works the 16th Conference of Young Researchers*, Military Technical Academy, pp. 133-140, 2021.
- [16] Kumeria, T., Santos, A., & Losic, D., "Nanoporous anodic alumina platforms: Engineered surface chemistry and structure for optical sensing applications", *Sensors*, 14(7), 11878-11918, 2014.
- [17] Pham, V. H., Nguyen, T. V., Nguyen, T. A., Pham, V. D., & Bui, H., "Nano porous silicon microcavity sensor for determination organic solvents and pesticide in water", *Advances in Natural Sciences: Nanoscience and Nanotechnology*, 5(4), 045003, 2014.
- [18] Kamble, A., Sinha, B., Chung, K., More, A., Vanalakar, S., Hong, C. W., et al. "Facile linker free growth of CdS nanoshell on 1-D ZnO: Solar cell application", *Electronic Materials Letters*, 11(2), 171-179, 2015.

PHÂN TÍCH UỐN TĨNH TẮM NANO HÌNH VÀNH KHUYÊN TRÊN NỀN ĐÀN HỒI SỬ DỤNG LÝ THUYẾT NONLOCAL

Tóm tắt: Bài báo trình bày thuật toán phân tử hữu hạn phân tích uốn tĩnh tấm FGP nano hình vành khuyên trên nền đàn hồi dựa trên lý thuyết nonlocal. Vật liệu FGP với hai tham số là chỉ số thể tích vật liệu (k) và hệ số thể tích lỗ rỗng (ζ) với hai trường hợp phân bố lỗ rỗng bao gồm phân bố đều và phân bố không đều. Nền đàn hồi bao gồm độ cứng Winkler (k_1) và độ cứng Pasternak (k_2). Lần đầu tiên, trường ứng suất và chuyển vị của tấm FGP nano hình vành khuyên được thiết lập bằng cách sử dụng phân tử tám nút ($Q8$). Kết quả tính toán số của phương pháp đề xuất được so sánh với các kết quả đã công bố để kiểm tra tính chính xác và độ tin cậy. Ngoài ra, ảnh hưởng của một số thông số nền và thuộc tính vật liệu đến uốn tĩnh của tấm FGM nano hình vành khuyên cũng được nghiên cứu chi tiết.

Từ khóa: FGM; uốn tĩnh; tấm nano; lý thuyết đàn hồi nonlocal.

Received: 05/07/2021; Revised: 29/07/2021; Accepted for publication: 02/08/2021

